Desalination and Water Treatment
www.deswater.com

doi: 10.5004/dwt.2019.23405

140 (2019) 268–282
February

Adsorption capability of surface-modified jujube seeds for Cd(II), Cu(II) and Ni(II) ions removal: mechanism, equilibrium, kinetic and thermodynamic analysis

R. Gayathri[a], K.P. Gopinath[b,*], P. Senthil Kumar[b,*], S. Suganya[b]

[a]*Tamilnadu Pollution Control Board, Guindy, Chennai 600032, India, Tel. +91 9894427191; email: gay3civil@gmail.com*
[b]*Department of Chemical Engineering, SSN College of Engineering, Chennai 603110, India, Tel. +91 9842739313; email: gopinathkp@ssn.edu.in (K.P. Gopinath), Tel. +91 9884823425; email: senthilchem8582@gmail.com (P. Senthil Kumar), Tel. +91 9159690215; email: sugish18@gmail.com (S. Suganya)*

Received 26 August 2018; Accepted 30 October 2018

ABSTRACT

In this work, the adsorption of metal ions (Cd(II), Cu(II) and Ni(II)) onto ultrasonic-modified jujube seeds (UMJS) was investigated in a batch mode system. The synthesized UMJS was analyzed using scanning electron microscopic and X-ray diffraction analyses to predict the adsorbent quality. The optimum condition for metal ions adsorption in the studied system is as follows: adsorbent dose = 2.4 g/L Cd(II) ions, 2 g/L Cu(II) ions and 3 g/L Ni(II) ions; temperature = 303 K; pH = 5.0; and contact time = 60 min. The two-parameter models (Langmuir and Freundlich) and three-parameter models (Redlich–Peterson and Toth) were used to delineate the removal rate of metal ions by the UMJS. Among tested isotherm models, Freundlich and Redlich–Peterson models produced the best fit ($R^2 > 0.99$) to the adsorption equilibrium data with low error values. Monolayer adsorption capacity of the UMJS for Cd(II), Cu(II) and Ni(II) was found to be 182.4, 259 and 140.9 mg/g, respectively. The thermodynamic results showed that the adsorption process is exothermic and spontaneous in nature. Adsorption kinetic was studied through pseudo-first-order and pseudo-second-order models where pseudo-first-order kinetic produced the best fit. From the results, UMJS can be used as a potential adsorbent for the removal of metal ions from wastewater.

Keywords: Jujube seeds; Adsorption; Isotherm; Kinetic; Thermodynamic; Exothermic

1. Introduction

Heavy metals in water cannot be visually detected, smelled or tasted. But the presence of excessive levels of heavy metal in drinking water is dangerous, tending to bioaccumulation in the environment. The ingression of heavy metals in aquatic systems by industrial or consumer waste, or from volcanic eruptions and acidic rain, can cause damage to blood composition, mental and central nervous function, vital organs, and long-term contact of heavy metals such as arsenic, cadmium, chromium, copper, nickel, lead and mercury in trace amounts can result in allergies [1]. In the note, long-term exposure to heavy metals can result in the culmination of neurological and degenerative processes as a mimic of Alzheimer's disease, Parkinson's disease and multiple sclerosis. Point source pollution of heavy metal can be identified unlike nonpoint pollution accommodates dispersed-source pollutant. Predominantly, mining industries are a source of commuting acid-soluble heavy metals in the freshwater ecosystems below pH 7.0, that is, favorable for metal solubility and mobility [2]. Therefore, metals are more toxic in soft water. Such high concentrations of dissolved metals are non-biodegradable. Indeed, dissolved metals cannot be

* Corresponding authors.

broken down dextrouslyinto less harmful components in the environment [3].

In contrast, some metals such as manganese, iron, copper and zinc are essential to living species as micronutrients, developed by the biological system is called "metal tolerance". However, essential minerals can also produce toxic effects at high concentrations [4,5]. Thus, the removal of heavy metal from the water stream becomes a prime concern. For which, carbon treatment is popular with high purity in the form of granules involving in ionization, oxidation and reduction processes that transform heavy metals to be less toxic and provides even more protection from bacterial growth. The huge surface area of activated carbon (AC) has countless bonding sites, in which, it attracts and holds the target compound from liquid streams, especially for the dilute concentrations of the contamination [6]. In case, if certain compounds escape or pass next to the carbon surface, they attach to the surface and are trapped. Therefore, trapping other carbon-based impurities is ease of access by AC as a great adsorbent. In specific, physical adsorption is encouraged for water adsorbates onto AC when their molecular size is smaller than the size of the carbon pore openings [7]. But the substance accumulation in the carbon pores can either be physical or chemical at the interface between the liquid and solid phases.

The qualities of AC rely in the type of raw material used, the length of the activation, the rate of reaction, the reaction temperature and the type of oxidizing agent. The carbonaceous source of jujube seeds (JS) was that choice of interest has become naturalized in tropical Africa, India, China and the Mediterranean, where it is commercially important. JS can be stored in a sealed container at 5°C for a year. Therefore, this work aims at the following: first, converting waste biomass, JS, into effective adsorbent with improved surface activity; second, optimizing preparation variables to achieve carbonization followed by dehydration, where the raw material results in the charring and amortization of the carbon, creating a porous structure and an extended surface area; and third, achieving pore distribution through ultrasonication post activation to impart additional physical activities. In regard, a low cost, environmentally friendly adsorbent from JS was demonstrated for adsorption of Cu(II), Cd(II) and Ni(II), respectively. The modeling of adsorption isotherms, kinetics and thermodynamic parameters was studied. A comprehensive appraisal of the removal of heavy metals by biomass-derived AC along with theoretical and mathematical expressions is well explained.

2. Materials and methods

2.1. Chemicals and reagents

All the chemicals and reagents used in experimental work are of analytical grade. The salts of copper sulfate pentahydrate, cadmium sulfate and nickel sulfate heptahydrate were purchased from Merck, India. Deionized water was used throughout the experiment.

2.2. Equipment

The pH of the prepared solution was calibrated using pH meter (HI 98107; Hanna Equipment Private Limited, Mumbai, India). The process of ultrasonication was carried out in a sonicator (VCX750, Sonics and Materials Inc., Newtown, USA). Drying in a hot air oven (Hasthas Scientific Instruments India (P) Ltd, Chennai, India) and batch adsorption studies in Orbital Incubation Shaker (Royal Testing Equipment, Chennai, India) were engaged. The percentage removal of the specific compound in the solution before and after adsorption was analyzed using atomic absorption spectrophotometer (AAS) (SL176 Model, Elico Limited, Chennai, India).

2.3. Conversion of waste biomass into surface-modified adsorbent

JS of current interest as raw material were collected from SSN College of Engineering, Chennai, India. Using distilled water, the collected seeds were washed and oven dried at 60°C for 2 h. Later, the dried seeds of interest were subjected to sieving with the particle size of 0.354 mm (42 mesh). The resultant is noted as "raw jujube seeds" (RJS).

2.3.1. Surface modification procedure

To achieve surface modification, sulfuric acid (H_2SO_4) as a chemical support or dehydrating agent was chosen. The mass per volume proportions of RJS and H_2SO_4 were 1:3 for the period of 24 h of incubation. The system was made sure that RJS is completely submerged in the acid to undergo dehydration, resulting in the charring and amortization of the carbon, creating a porous structure and an extended surface area. Surface activity of RJS can be controlled by adding up the higher concentration of H_2SO_4. After a stipulated period, the system was washed with dH_2O, until the pH gets neutralized, and dried at 80°C for 3 h. The resultant is noted as "sulfuric acid-modified jujube seeds" (SMJS).

Pore distribution is a prime concern in good adsorbent, hence it is achieved through ultrasonication. In spite of the process "acid wash" is involved in the purification of AC post activation, additional physical properties were developed through sonication by placing SMJS:dH_2O mixture (1:10 m/v ratio) at 24 kHz working frequency with the speed of 500 rpm for 20 min. After sonication, the mixture was withdrawn, filtered and dried at 80°C for 4 h. The resultant is noted as "ultrasonic-modified jujube seeds" (UMJS).

2.4. Characterization of adsorbents

The adapted materials (RJS, SMJS and UMJS) were characterized using scanning electron microscopy (SEM) using electron probe micro-analyzer (Model Jeol-JXA 840 A, Japan). During morphological studies, no coating material was applied to the specimen. A crystallographic nature of the material was studied through X-ray powder diffractometry (XRD) using a Siemens D5000 XRD with copper radiation and a scintillation detector.

2.5. Setup for batch adsorption experiments

2.5.1. Preparation of metal ion solution

A stock solution of Cd(II), Cu(II) and Ni(II) metal solution was prepared by dissolving appropriately weighed respective salt in 1 L of distilled water. Dilution was performed by

adding dH_2O to the desired concentration of the working solution of adsorbate. The pH of the solution was testified and adjusted by adding 0.01 M of NaOH or HCl.

2.5.2. Batch adsorption procedure

The removal of different metal ions from the aqueous solution was performed to study the equilibrium adsorption by adding the known quantity of UMJS to 100 mL of prepared metal ion concentration in 100 mL Erlenmeyer flasks at 303 K for pH 5.0.Adsorption period was varied from 10 to 90 min for each set of experiments while changing the parameters such as initial metal ion concentration and temperature at the agitation speed of 80 rpm. After incubation, the adsorption mixtures were filtered using Whatman 42 filter paper. The concentration of the final metal ion from the supernatant was measured by an AAS (SL 176 Model, Elico Limited, Chennai, India).

The following formula was used to determine the percentage removal of metal ions:

$$\text{Removal percentage of metal ion} = \frac{C_o - C_e}{C_o} \times 100 \quad (1)$$

where C_o and C_e are the initial and equilibrium concentrations (mg/L) of metal ions, respectively.

2.6. Isotherm modeling

The equilibrium isotherm data were studied through the nonlinear isotherm models such as Langmuir [8], Freundlich [9], Redlich–Peterson [10] and Toth isotherm models [11]. The fitness of these models was evaluated by the determination of nonlinear coefficient of correlation (R^2) and error values. Computing was carried out using MatlabR2009a software package to inspect R^2 and error values. It happens at the specific homogeneous site for the successful application of monolayer adsorption.

Langmuir isotherm is expressed as follows:

$$q_e = \frac{q_m K_L C_e}{1 + K_L C_e} \quad (2)$$

where q_e is the quantity of metal ions adsorbed (mg/g), q_m is the maximum monolayer adsorption capacity (mg/g), and K_L is the Langmuir adsorption constant related to the affinity of the metal ions to the adsorbent (L/mg).

The Freundlich model deviates from the Langmuir model of adsorption. In the Freundlich model, the rate of adsorption varies directly as the amount of gas adsorbed by the adsorbent with pressure at constant temperature.

The Freundlich model is expressed as follows:

$$q_e = K_F C_e^{1/n} \quad (3)$$

where K_F is the Freundlich constant ([mg/g][L/mg]$^{1/n}$) used to measure the adsorption capacity and n is the Freundlich exponent which is used to measure the intensity of adsorption. The consequence of n is given as follows: $n = 1$ (linear), $n > 1$ (physical process), and $n < 1$ (chemical process).

Redlich–Peterson and Toth isotherms are the three-parameter equations used in the isotherm studies.

The Redlich–Peterson model is expressed as follows:

$$q_e = \frac{K_{RP} C_e}{1 + \alpha_{RP} C_e^{\beta_{RP}}} \quad (4)$$

where α_{RP} is the Redlich–Peterson isotherm constant $(L/mg)^{1/\beta_{RP}}$, K_{RP} is Redlich–Peterson isotherm constant (L/g), and β_{RP} is the exponent which lies between 0 and 1. The significance of 'β' is given by as follows:

$\beta = 0$, Freundlich adsorption isotherm model is a preferable adsorption isotherm model; and $\beta = 1$, Langmuir adsorption isotherm model is a preferable adsorption isotherm model.

Toth model equation is expressed as follows:

$$q_e = \frac{q_{mT} C_e}{\left(\frac{1}{K_T} + C_e^{mT}\right)^{\frac{1}{mT}}} \quad (5)$$

where q_e is the adsorbed amount of metal ion at equilibrium (mg/g), q_{mT} is the Toth maximum adsorption capacity (mg/g), C_e is the adsorbate equilibrium concentration (mg/L), K_T is the Toth equilibrium constant, and mT is the Toth model exponent.

2.7. Kinetic modeling and mechanism

Adsorption kinetic study was performed by taking an adsorption mixture of 100 mL each metal ion namely Cd(II), Cu(II) and Ni(II) with various amount (2.4, 2.0 and 3.0 g) of UMJS, respectively, by varying the contact time (10–60 min) for an initial metal ion concentration = 100 mg/L and at an optimum condition. The samples were taken from the solution for analyzing at fixed time intervals. After the predetermined time interval, the spent adsorbent material was separated by filtration using Whatman 42 filter paper, and the final concentration of each metal ion in the residual solution was measured by employing an AAS.

The number of metal ions adsorbed at different time interval q_t (mg/g) was calculated using the following formula:

$$q_t = \frac{(C_o - C_t)V}{m} \quad (6)$$

where q_t is the amount of metal ions adsorbed onto the adsorbent at any time t (mg/g), C_o is the initial concentration of metal ions (mg/L), C_t is the concentration of metal ions measured at time interval t (mg/L), m is the mass of the adsorbent (g), and V is the volume of the metal ions solution (L).

Kinetic models of pseudo-first-order, pseudo-second-order and intraparticle diffusion models were fit with the experimental data to determine the adsorption rate.

Pseudo-first-order kinetic model equation is expressed as follows:

$$q_t = q_e(1-\exp(-k_1 t)) \quad (7)$$

where k_1 is the pseudo-first-order kinetic rate constant (min^{-1}) and t is the time (min).

Pseudo-second-order kinetic model equation is expressed as follows:

$$q_t = \frac{q_e^2 k_2 t}{1 + q_e k_2 t} \quad (8)$$

where t is the time (min), and k_2 is the pseudo-second-order kinetic rate constant (g/mg min).

The intraparticle diffusion model is expressed as follows

$$q_t = k_p t^{1/2} + C \quad (9)$$

where q_t is the adsorption capacity at time t (mg/g), k_p is the intraparticle diffusion rate constant (mg/g $min^{1/2}$), t is the time (min), and C is the intercept.

2.8. Thermodynamic modeling

The thermodynamic parameters such as enthalpy ($\Delta H°$, kJ/mol), entropy ($\Delta S°$, kJ/mol) and Gibbs free energy ($\Delta G°$, kJ/mol) were used to study the adsorption characteristics and to identify the nature of adsorption process. These parameters can be intended from the following expressions:

$$K_c = \frac{C_{Ae}}{C_e} \quad (10)$$

$$\Delta G° = -RT \ln K_c \quad (11)$$

$$\Delta G° = \Delta H° - T\Delta S° \quad (12)$$

$$\text{Log } K_c = \frac{\Delta S°}{2.303R} - \frac{\Delta H°}{2.303RT} \quad (13)$$

where C_e is the equilibrium concentration in solution (mg/L), C_{Ae} is the amount of metal ion adsorbed on the adsorbent per liter of solution at equilibrium (mg/L), R is the gas constant (8.314 J/mol K), T is the temperature (K), and K_c is the equilibrium constant. The values of $\Delta H°$ and $\Delta S°$ were calculated from the slope and the intercept of the plot of log K_c vs. $1/T$.

3. Results and discussion

3.1. Characteristics of adsorbents

3.1.1. SEM analysis

SEM analysis was performed by focusing electron beam over a surface of the RJS, SMJS and UMJS to create an image. The shape of objects and spatial variations in chemical compositions have been identified and presented in Figs. 1(a)–(c).

SEM micrographs of the RJS show no or poorly developed pores [12], while in the surface-modified samples (Figs. 1(b) and (c)), a highly developed pore structure can be visible. It is evident that H_2SO_4 activation ensures enough

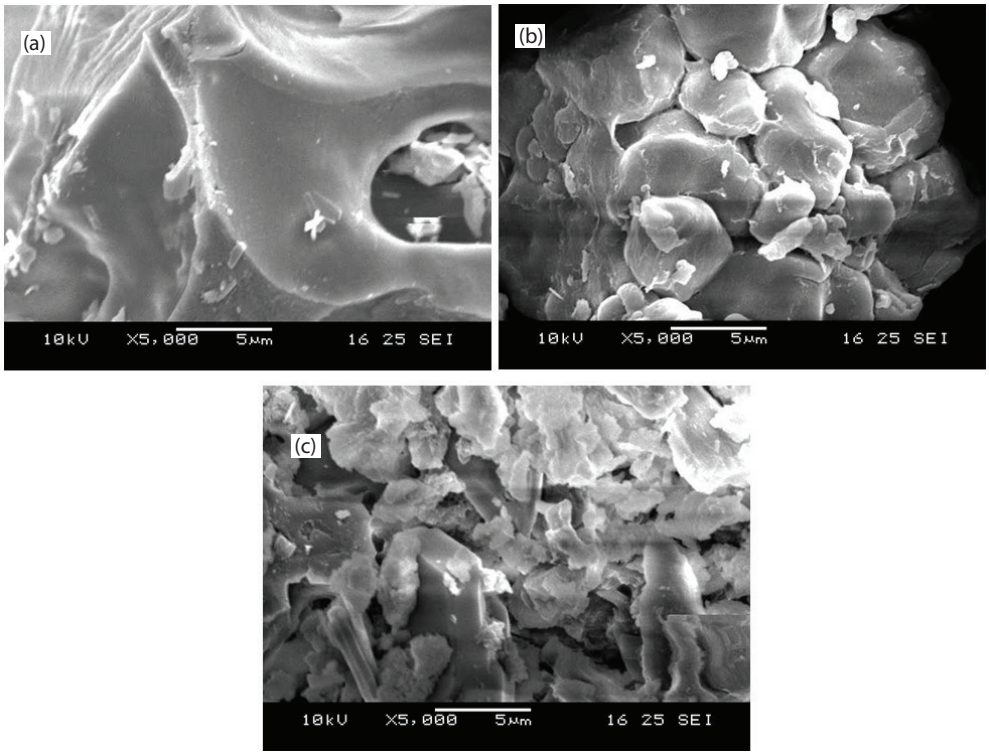

Fig. 1. SEM micrographs of (a) RJS, (b) SMJS and (c) UMJS.

pore distribution to be used as an adsorbent without further treatment. Yet, ultrasonication of SMJS has offered narrow dispersion [13] to carbon specimen with the particle size of 5 μm. Such chemically derived adsorbent (UMJS) seems to be spherical, aggregated with a slight change in the size of the pieces [14]. Both surface-modified carbon specimens resulted in cracks and crevices with developed pores.

3.1.2. XRD analysis

XRD images of RJS and UMJS are shown in Figs. 2(a) and (b). The amorphous nature [15] of RJS was confirmed by the less intense peaks, resulting in 2θ = 16.1° and 70.1° in Fig. 2(a). After surface modification, the UMJS resulted in high intense peaks as an indication of an increase in pore size and surface area development [16]. The *X*–*Y* peaks were found at 2θ = 28.324° and 62.3° because of acid treatment causing disappearance of major peaks due to leaching out minerals from RJS during activation and later washing with dH_2O. However, minor peaks at 28.324°, resulting in the formation of minerals during neutralization of the produced carbon [17], could react with the remaining lignocellulose in the final carbon yielded.

3.2. Effect of adsorption parameters

3.2.1. The initial metal ion concentration

There are several parameters influencing the adsorption behavior of UMJS, type of metal ion being treated, sufficiency in surface area, number of active sites created by the functional groups and selectivity of adsorbent. In adsorption, a lower to a higher concentration of metal ion is suggested to exhibit total saturation of adsorbent [18]. The initial concentration of 50–500 mg/L for Cd(II), Cu(II) and Ni(II) with the constant dose of 2.4, 2 and 3 g/L adsorbent was taken. In Figs. 3(a)–(c), the removal rate of Cd(II), Cu(II) and Ni(II) is shown to be declined from 99.38% to 84.22%, from 99.42% to 88.79% and from 99.18% to 81.75%, respectively. In the note, the decline occurred with the increase in metal ion concentration owing to the decrease in adsorption capacity of adsorbent. Because mass transfer between the metal ions and solid adsorbent in the aqueous solution becomes raised as the metal ions subsequently adsorbed onto the mass of adsorbent increased [19]. At higher concentration, the saturation of active sites of adsorbent occurs, resulting in the less occupancy by metal ions.

3.2.2. Contact time

As a function of contact time, the removal rate of Cd(II), Cu(II) and Ni(II) onto UMJS was calculated. In Figs. 4(a)–(c), it can be seen that the reaction mixture having pH 5.0 attained equilibrium at 60 min, initially set from 10 to 90 min at 303 K. After the point of saturation, the removal rate was found to be increasing until obtaining a steady state [20]. Undeniably, the occupancy of active sites by metal ions or mass transfer becomes high at the increased time. The removal percentage noted at equilibrium was 99.387%, 99.428% and 99.189% for Cd(II), Cu(II) and Ni(II), respectively. Equilibrium at 60 min is logical and maintained for further experiments.

3.2.3. Temperature

Heat evaluation in adsorption is a key component to study the extent of adsorption at constant pressure. The performance of a change in temperature from 303 K to 333 K

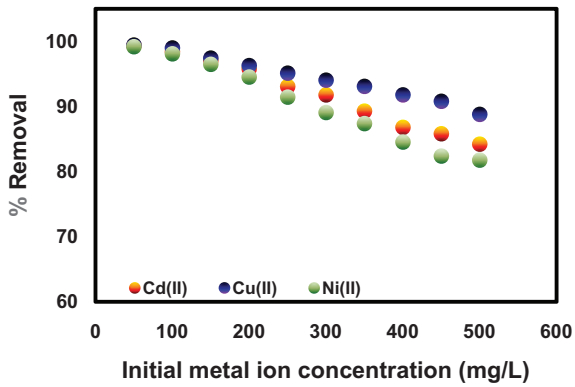

Fig. 3. Effect of initial metal ion concentration over the percentage removal of metal ions (adsorbent dose = 2.4 g/L [Cd(II)], 2 g/L [Cu(II)] and 3 g/L [for Ni(II)]; initial metal ion concentration = 50–500 mg/L; pH = 5.0; time = 60 min; and temperature = 303 K).

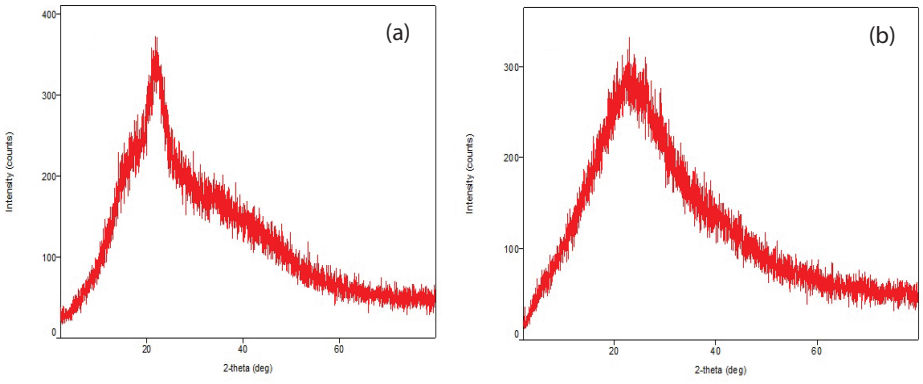

Fig. 2. XRD micrographs of (a) RJS and (b) UMJS.

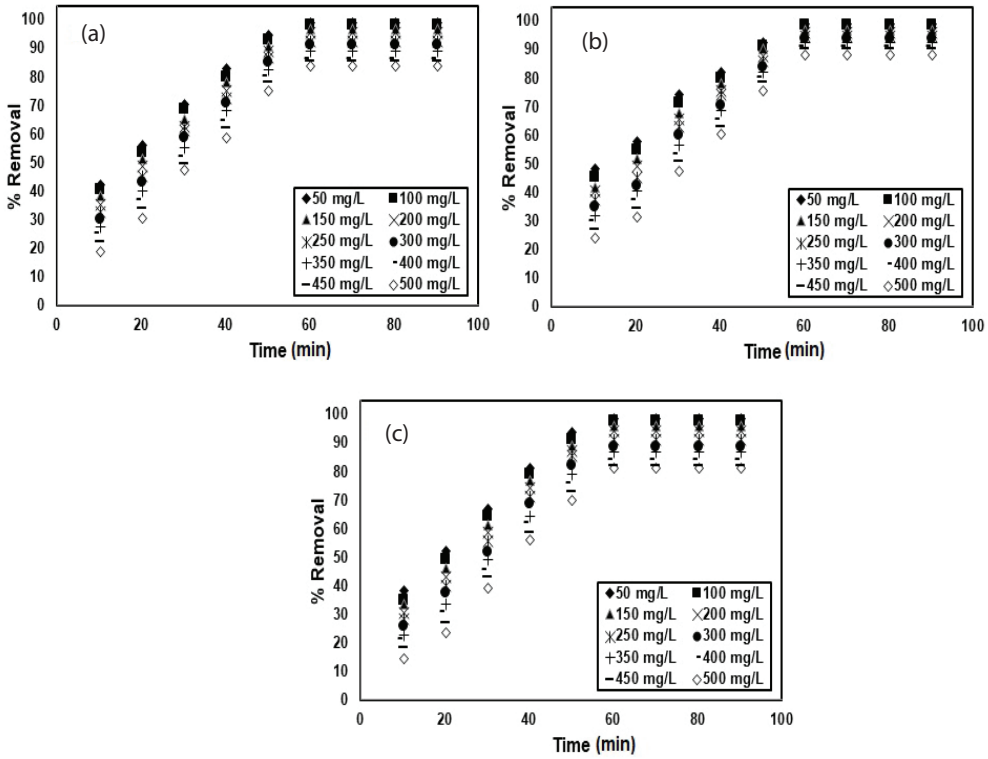

Fig. 4. Effect of contact time over the percentage removal of (a) Cd(II), (b) Cu(II) and (c) Ni(II) ions (adsorbent dose = 2.4 g/L [Cd(II)], 2 g/L [Cu(II)] and 3 g/L [Ni(II)]; initial metal ion concentration = 50–500 mg/L; pH = 5.0; time = 10–90 min; and temperature = 303 K).

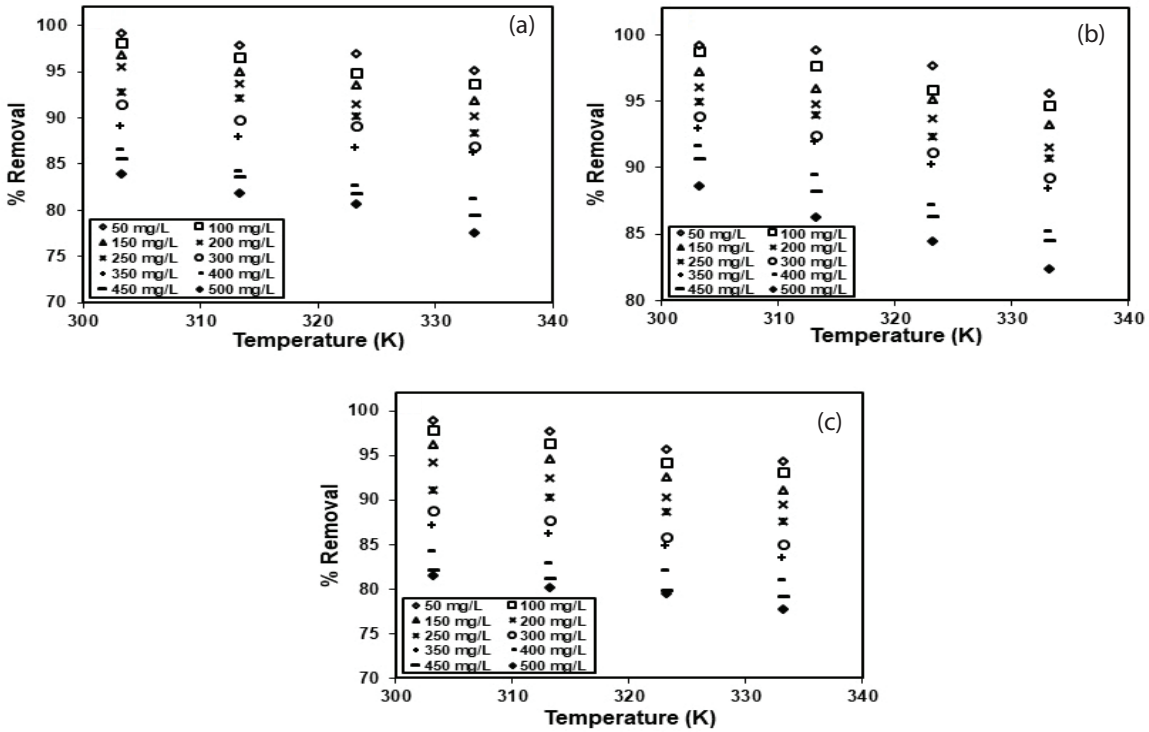

Fig. 5. Effect of temperature over the percentage removal of (a) Cd(II), (b) Cu(II) and (c) Ni(II) ions (adsorbent dose = 2.4 g/L [Cd(II)], 2 g/L [Cu(II)] and 3 g/L [Ni(II)]; initial metal ion concentration = 50–500 mg/L; pH = 5.0; time = 60 min; and temperature = 303–333 K).

for 50 to 500 mg/L metal ion concentration revealed that the rise in adsorption rate is high at low temperature, while high temperature leads to gradual lesser removal, because exothermic adsorption process is possible while the surface activity of adsorbent at high temperature requires more energy to let adsorbent stay in the liquid medium (Fig. 5). Therefore, the removal rate of Cd(II), Cu(II) and Ni(II) was found to be declined from 99.38% to 84.22%, from 99.42% to 88.79% and from 99.18% to 81.75%, respectively. The increase in temperature leads to the decrease in adsorbent density [21], hence proved by the removal percentage. In any case, JS can be used as a potential adsorbent in the reduction of heavy metal ions in wastewater.

3.3. Thermodynamic parameters

Gibbs free energy ($\Delta G°$), the enthalpy ($\Delta H°$) and the entropy ($\Delta S°$) are the thermodynamic parameters, which enable us to understand whether the particular adsorption process is physical or chemical, spontaneous or non-spontaneous and also exothermic or endothermic. From the experimental data, the plot log K_c vs. $1/T$ (Figs. 6(a)–(c)) was drawn to discern Gibbs free energy, a driving force, a relationship between the free solute compound at the initial state and the adsorbed compound at equilibrium state. Furthermore, the distribution coefficient, that is, equilibrium constant was determined to find the change in enthalpy and entropy. From these thermodynamic parameters,

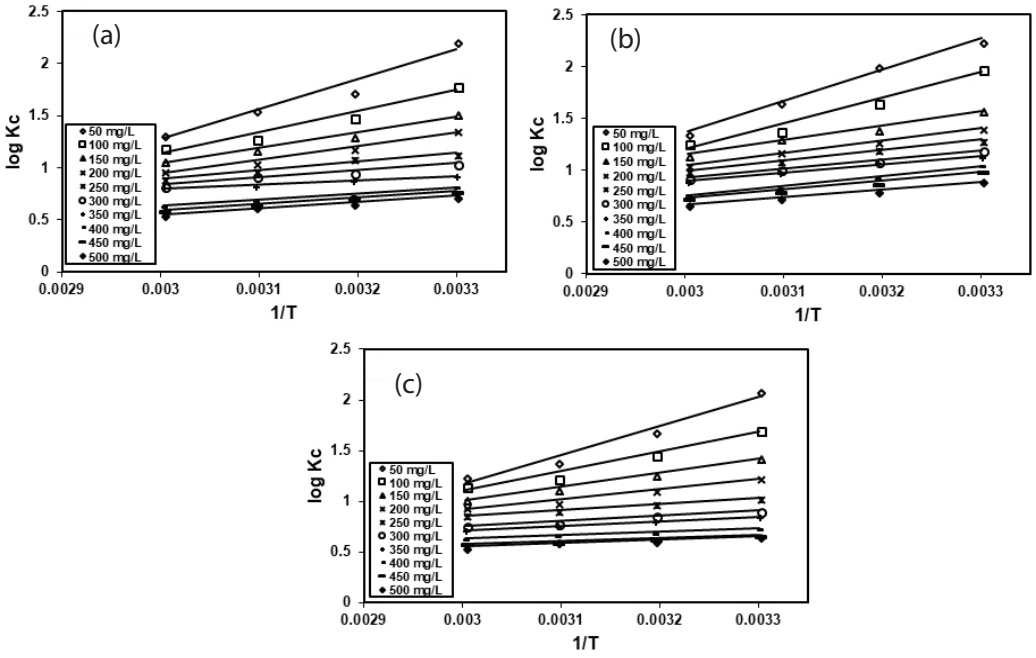

Fig. 6. Thermodynamic analysis on the removal of (a) Cd(II), (b) Cu(II) and (c) Ni(II) ions (adsorbent dose = 2.4 g/L [Cd(II)], 2 g/L [Cu(II)] and 3 g/L [Ni(II)]; initial metal ion concentration = 50–500 mg/L; pH = 5.0; time = 60 min; and temperature = 303–333 K).

Table 1
Thermodynamic parameters for the removal of Cd(II)ions

C_o (mg/L)	$\Delta H°$ (kJ/mol)	$\Delta S°$ (J/mol/K)	($\Delta G°$) (kJ/mol)			
			303 K	313 K	323 K	333 K
50	–55.086	–140.846	–12.820	–10.324	–9.628	–8.412
100	–38.843	–94.663	–10.412	–8.940	–7.975	–7.625
150	–28.552	–65.598	–8.823	–7.799	–7.291	–6.829
200	–25.008	–56.847	–7.872	–7.140	–6.481	–6.216
250	–15.787	–30.156	–6.546	–6.505	–6.027	–5.687
300	–13.198	–23.551	–6.082	–5.732	–5.716	–5.300
350	–76.05	–7.5631	–5.341	–5.215	–5.107	–5.130
400	–11.201	–21.444	–4.744	–4.419	–4.247	–4.094
450	–12.100	–24.929	–4.535	–4.291	–4.068	–3.775
500	–11.180	–22.919	–4.221	–3.974	–3.883	–3.480

Table 2
Thermodynamic parameters for the removal of Cu(II) ions

C_o (mg/L)	$\Delta H°$ (kJ/mol)	$\Delta S°$ (J/mol/K)	($\Delta G°$) (kJ/mol)			
			303 K	313 K	323 K	333 K
50	57.705	–146.935	–7.538	–11.991	–10.263	–8.647
100	47.588	–119.65	–11.542	–9.973	–8.565	–8.067
150	26.407	–57.135	–9.157	–8.357	–8.095	–7.342
200	23.007	–48.863	–8.196	–7.669	–7.336	–6.673
250	19.079	–38.122	–7.481	–7.217	–6.742	–6.363
300	17.105	–33.526	–6.952	–6.568	–6.321	–5.916
350	15.782	–30.271	–6.551	–6.399	–6.007	–5.664
400	18.171	–40.017	–6.080	–5.614	–5.193	–4.893
450	16.152	–34.484	–5.765	–5.268	–5.030	–4.724
500	14.205	–29.793	–5.214	–4.816	–4.583	–4.304

Table 3
Thermodynamic parameters for the removal of Ni(II) ions

C_o (mg/L)	$\Delta H°$ (kJ/mol)	$\Delta S°$ (J/mol/K)	($\Delta G°$) (kJ/mol)			
			303 K	313 K	323 K	333 K
50	55.118	–142.895	–12.110	–10.104	–8.564	–7.916
100	36.921	–89.6125	–9.921	–8.778	–7.653	–7.343
150	26.704	–60.849	–8.611	–7.598	–6.920	–6.548
200	19.468	–40.840	–7.416	–6.635	–6.097	–6.016
250	11.028	–16.619	–5.967	–5.885	–5.620	–5.499
300	9.957	–15.394	–5.289	–5.183	–4.899	–4.873
350	8.575	–12.120	–4.872	–4.822	–4.662	–4.518
400	6.396	–7.046	–4.280	–4.154	–4.129	–4.056
450	6.179	–7.907	–3.887	–3.831	–3.724	–3.725
500	6.179	–7.907	–3.779	–3.676	–3.694	–3.506

Table 4
Adsorption isotherm parameters for the removal of Cd(II) ions

Isotherm model	Parameter	R^2	SSE	RMSE
Langmuir	q_m = 182.4 (mg/g)	0.9421	1,401	13.23
	K_l = 0.0872 (L/mg)			
Freundlich	n = 2.729	0.9977	56.82	2.665
	K_F = 34.89 ([mg/g]/[L/mg]$^{(1/n)}$)			
Redlich–Peterson	α_{RP} = 1.086 (L/mg)	0.9897	250.3	5.593
	β_{RP} = 0.7241			
	K_{RP} = 52.82			
Toth	α_T = 11.46 (L/mg)	0.9421	1,401	14.15
	K_T = 41.89			
	n = 0.2296			

thermodynamic feasibility, spontaneity and thermal effects of sorption can be determined. From Tables 1–3, the negative values presented in $\Delta G°$, $\Delta H°$ and $\Delta S°$ resulted in the release of energy while metal ions were attracted on the surface of adsorbent, which is $\Delta H°$ dependent [22]. This is the reason for the heat of adsorption to be negative or exothermic. The negative values of $\Delta G°$ at various temperatures had shown the spontaneous nature of adsorption.

A combination of physical or chemical adsorptions can occur during the interaction between the adsorbate and the surface of adsorbent via hydrogen bond or ligand exchange. In this study, both physical and chemical adsorptions were observed in the removal of Cd(II), Cu(II) and Ni(II) onto UMJS. The negative values in entropy change seem to be decreased with respect to the change in occupancy of active sites [23]. Adsorption is further confirmed by the negative values of $\Delta G°$ ($\Delta G° = \Delta H° – T\Delta S°$).

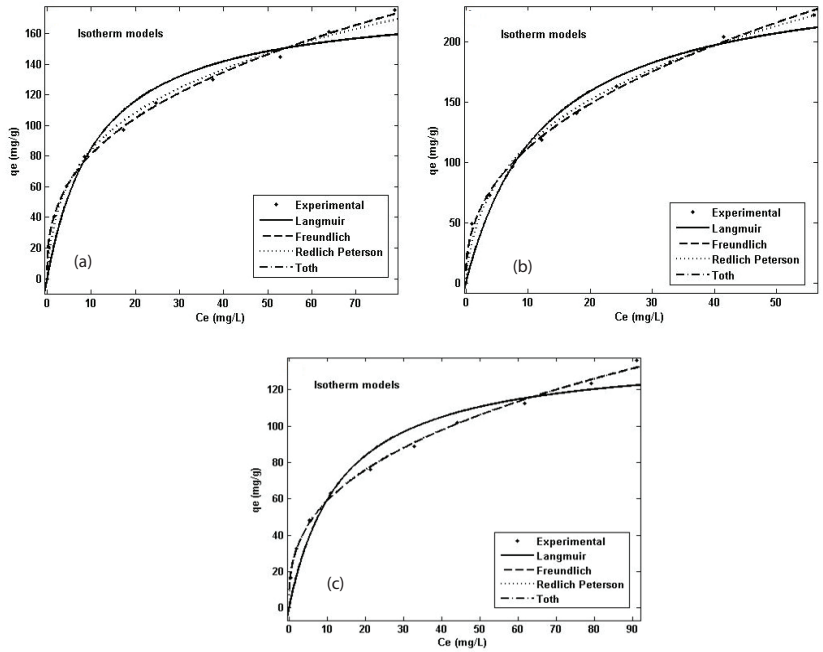

Fig. 7. Adsorption isotherm fit for the removal of (a) Cd(II), (b) Cu(II) and (c) Ni(II) ions (adsorbent dose = 2.4 g/L [Cd(II)], 2 g/L [Cu(II)] and 3 g/L [Ni(II)]; initial metal ion concentration = 50–500 mg/L; pH = 5.0; time = 60 min; and temperature = 303 K).

Table 5
Adsorption isotherm parameters for the removal of Cu(II) ions

Isotherm model	Parameter	R^2	SSE	RMSE
Langmuir	q_m = 259 (mg/g)	0.9543	1,831	15.13
	K_l = 0.0794 (L/mg)			
Freundlich	n = 2.443	0.9975	99.86	3.533
	K_F = 43.53 ([mg/g]/[L/mg]$^{(1/n)}$)			
Redlich–Peterson	α_{RP} = 1.892 (L/mg)	0.9985	460.9	7.59
	β_{RP} = 0.6891			
	K_{RP} = 67.39			
Toth	α_T = 12.58 (L/mg)	0.9543	1,831	16.17
	K_T = 36.17			
	n = 0.1396			

Table 6
Adsorption isotherm parameters for the removal of Ni(II)ions

Isotherm model	Parameter	R^2	SSE	RMSE
Langmuir	q_m = 140.9 (mg/g)	0.9359	914.6	10.69
	K_l = 0.073 (L/mg)			
Freundlich	n = 2.726	0.9972	40.68	2.255
	K_F = 25.27 ([mg/g]/[L/mg]$^{(1/n)}$)			
Redlich–Peterson	α_{RP} = 33.73 (L/mg)	0.9972	40.24	2.398
	β_{RP} = 0.6372			
	K_{RP} = 868.6			
Toth	α_T = 13.68 (L/mg)	0.9359	914.6	11.43
	K_T = 54.97			
	n = 0.3901			

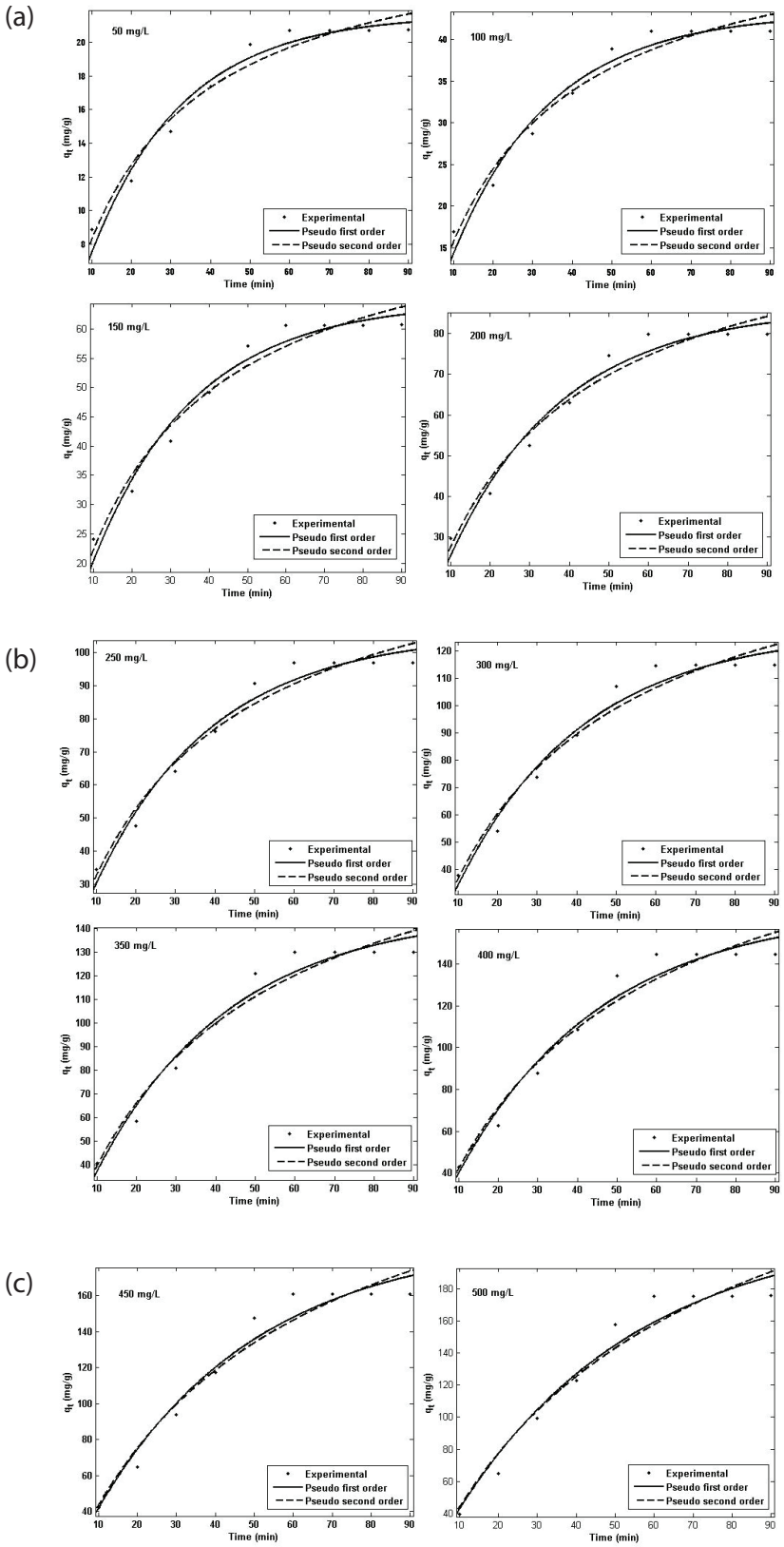

Fig. 8. Adsorption kinetic model fit for the removal of Cd(II) ions: (a) adsorbent dose = 2.4 g/L, initial metal ion concentration = 50–200 mg/L, pH = 5.0, time = 10–90 min and temperature = 303 K; (b) adsorbent dose = 2.4 g/L, initial metal ion concentration = 250–400 mg/L, pH = 5.0; time = 10–90 min and temperature = 303 K; and (c) adsorbent dose = 2.4 g/L, initial metal ion concentration = 450–500 mg/L, pH = 5.0, time = 10–90 min and temperature = 303 K.

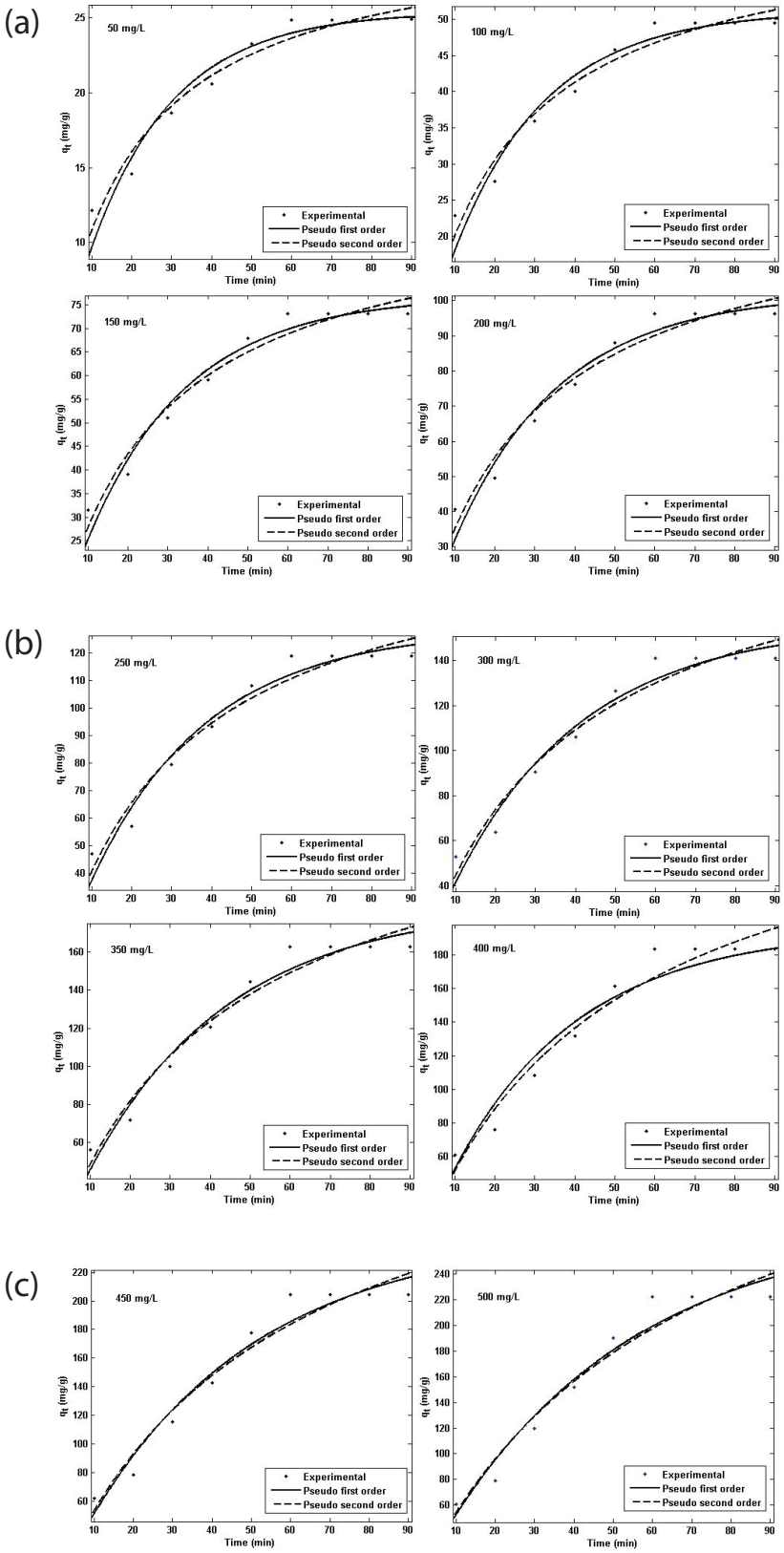

Fig. 9. Adsorption kinetic model fit for the removal of Cu(II) ions: (a) adsorbent dose = 2 g/L, initial metal ion concentration = 50–200 mg/L, pH = 5.0, time = 10–90 min and temperature = 303 K; (b) adsorbent dose = 2 g/L, initial metal ion concentration = 250–400 mg/L, pH = 5.0, time = 10–90 min and temperature = 303 K; and (c) adsorbent dose = 2 g/L, initial metal ion concentration = 450–500 mg/L, pH = 5.0, time = 10–90 min and temperature = 303 K.

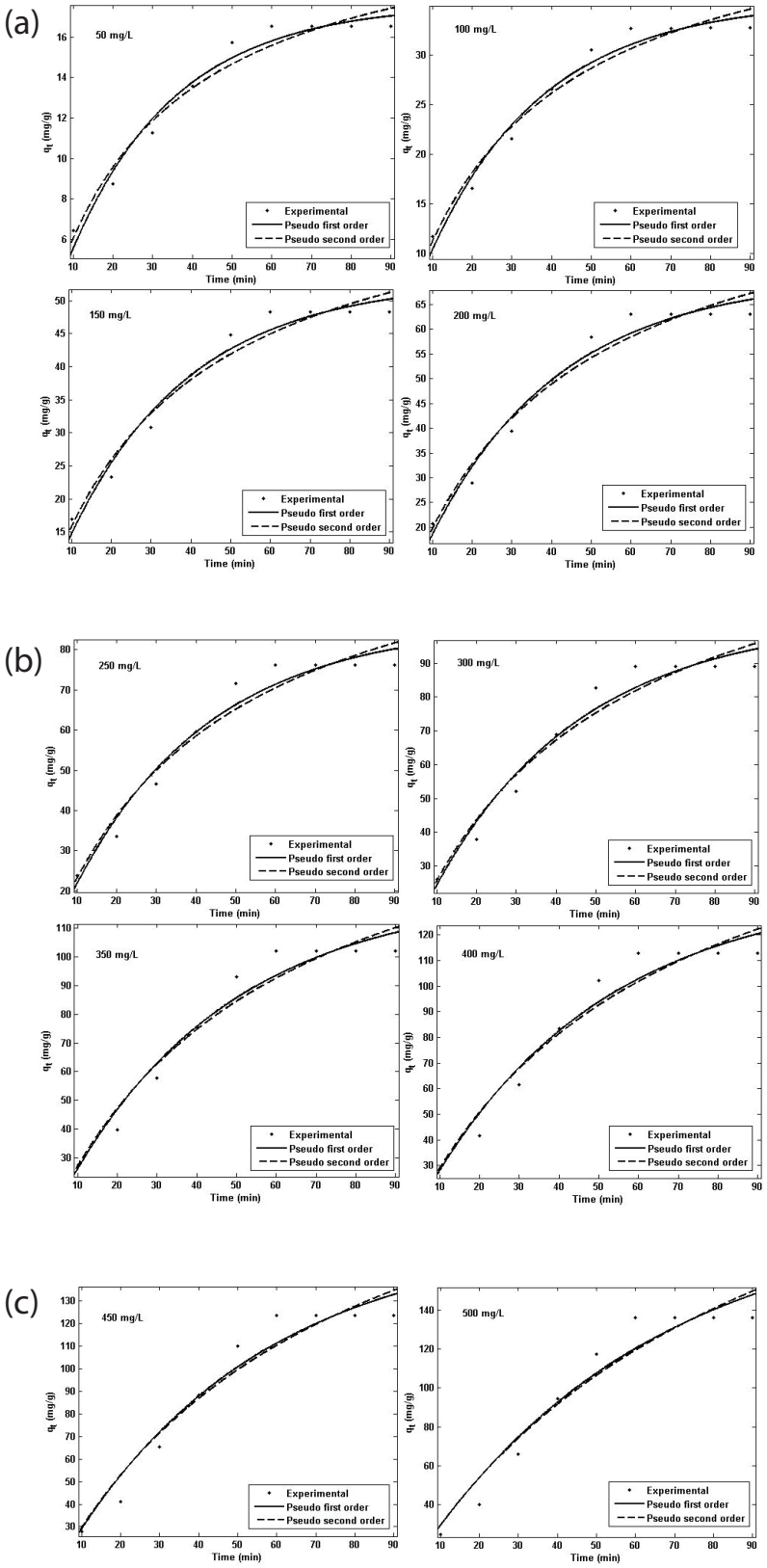

Fig. 10. Adsorption kinetic model fit for the removal of Ni(II) ions: (a) adsorbent dose = 3 g/L, initial metal ion concentration = 50–200 mg/L, pH = 5.0, time = 10–90 min and temperature = 303 K; (b) adsorbent dose = 3 g/L, initial metal ion concentration = 250–400 mg/L; pH = 5.0, time = 10–90 min and temperature = 303 K; and (c) adsorbent dose = 3 g/L, initial metal ion concentration = 450–500 mg/L, pH = 5.0, time = 10–90 min and temperature = 303 K.

Table 7
Adsorption kinetics and diffusion mechanism parameters for the removal of Cd(II) ions

C_o (mg/L)	q_e (exp)	Pseudo-first-order			Pseudo-second-order			Intraparticle diffusion		
		k_1 (min^{-1})	q_e (mg/g)	R^2	k_2 (min^{-1})	q_e (mg/g)	R^2	k_p (mg/g min$^{(1/2)}$)	R^2	C
50	21.35	0.0428	21.62	0.9712	0.0016	27.13	0.9669	2.0241	0.9126	3.5399
100	43.05	0.0402	43.18	0.9725	0.0007	54.87	0.9679	4.1498	0.92	5.6941
150	64.42	0.0377	64.61	0.9711	0.0004	83.29	0.9654	6.3607	0.9228	6.4457
200	86.18	0.0348	86.29	0.9734	0.0002	113.3	0.9661	8.7414	0.9267	5.1455
250	105.8	0.0335	105.8	0.975	0.0002	140.6	0.9653	10.914	0.9237	3.8402
300	127.32	0.0313	127.4	0.9748	0.0001	172.6	0.9639	13.445	0.9241	0.0059
350	147.15	0.0293	147.2	0.9718	0.0001	202.7	0.9609	15.754	0.9246	4.3798
400	166.54	0.0274	166.6	0.969	0.00009	233.5	0.9582	18.041	0.9255	9.6417
450	191.88	0.0245	191.9	0.9666	0.00006	277.1	0.9565	21.088	0.9292	19.821
500	218.74	0.0216	218.8	0.9633	0.00004	326.8	0.9543	24.189	0.9335	32.324

Table 8
Adsorption kinetics and diffusion mechanism parameters for the removal of Cu(II) ions

C_o (mg/L)	q_e (exp)	Pseudo-first-order			Pseudo-second-order			Intraparticle diffusion		
		k_1 (min^{-1})	q_e (mg/g)	R^2	k_2 (min^{-1})	q_e (mg/g)	R^2	k_p (mg/g min$^{(1/2)}$)	R^2	C
50	25.354	0.0480	25.39	0.9475	0.0017	30.97	0.9619	2.2147	0.9256	5.9506
100	51.154	0.0435	51.17	0.9533	0.0007	63.62	0.9616	4.6827	0.93	9.3831
150	76.75	0.0399	76.79	0.9628	0.0004	97.41	0.963	7.3258	0.9275	10.421
200	131.04	0.0002	131	0.9612	0.0376	102.1	0.9609	9.9221	0.9327	11.082
250	128.25	0.0343	128.6	0.9642	0.0001	168.9	0.9598	12.924	0.9307	7.9183
300	156.18	0.0308	156.2	0.9625	0.0001	210.2	0.9576	16.073	0.9342	2.5121
350	184.56	0.0283	184.5	0.9671	0.00009	254	0.9608	19.369	0.9376	4.23
400	195.45	0.0316	195.5	0.9501	0.00006	300.4	0.9561	22.566	0.9367	11.662
450	246.52	0.0236	246.6	0.9616	0.00004	357.5	0.9548	26.287	0.9369	23.472
500	280.05	0.0207	280.1	0.9602	0.00003	419	0.9534	29.89	0.9376	37.255

Table 9
Adsorption kinetics and diffusion mechanism parameters for the removal of Ni(II) ions

C_o (mg/L)	q_e (exp)	Pseudo-first-order			Pseudo-second-order			Intraparticle diffusion		
		k_1 (min^{-1})	q_e (mg/g)	R^2	k_2 (min^{-1})	q_e (mg/g)	R^2	k_p (mg/g min$^{(1/2)}$)	R^2	C
50	17.588	0.0378	17.64	0.9738	0.0015	22.77	0.9649	1.7458	0.9155	1.6975
100	35.340	0.0348	35.44	0.9779	0.0006	46.74	0.9676	3.6275	0.9216	1.8048
150	52.90	0.0327	52.99	0.9731	0.0004	70.86	0.963	5.4993	0.9229	1.3068
200	70.46	0.0305	70.46	0.9727	0.0002	95.99	0.9617	7.4641	0.9237	0.6983
250	86.52	0.0290	86.52	0.9671	0.0002	119.6	0.9551	9.2929	0.9179	3.0079
300	103.25	0.0275	103.2	0.966	0.0004	145.4	0.9546	11.226	0.9216	6.8133
350	122.4	0.0241	122.4	0.9639	0.0001	177.7	0.9537	13.449	0.9273	13.342
400	138.4	0.0223	138.4	0.9591	0.00008	204.2	0.9494	15.211	0.926	17.801
450	158.86	0.0201	158.9	0.9556	0.00005	242	0.9471	17.432	0.9295	26.286
500	190.68	0.0166	190.7	0.9486	0.00003	304.9	0.9421	20.407	0.9338	39.799

3.4. Adsorption isotherm

The active sites of UMJS undergoing adsorption were analyzed as a function of adsorption capacity, whereas Langmuir and Freundlich isotherm models (two-parameter models) and Redlich–Peterson and Toth isotherm models (three-parameter models) were used. Table 4 shows the consolidated report of the correlation coefficients R^2 values for both models on the removal of Cd(II). The slope and intercept of the linear plot in Fig. 7(a) presents $R^2 > 0.9421$ and 0.9977 (two-parameter models); $R^2 >$ 0.9897 and 0.9421 (three-parameter models), respectively. It can be said that Freundlich and Redlich–Peterson models fit the experimental data well with low error values. Significantly, the adsorption capacity (q_m) of UMJS is 182.4 mg/g.

Similarly, Table 5 presents $R^2 > 0.9543$ and 0.9975 (two-parameter models); $R^2 > 0.9985$ and 0.9543 (three-parameter models) for the removal of Cu(II) with the adsorption capacity of 259 mg/g. In extension, Table 6 presents $R^2 > 0.9359$ and 0.9972 (two-parameter models); $R^2 >$ 0.9359 and 0.9972 (three-parameter models) for the removal of Ni(II) with the adsorption capacity of 140.9 mg/g. On the whole, Freundlich and Redlich–Peterson models fit the experimental data well with low error values [24,25].

In general, monolayer adsorption is well explained by Langmuir isotherm as the affinity between the molecules becomes high. Besides, size and shape of the adsorbent are even and responsible for the equal affinity of metal particles, resulting in a homogenous nature [26].In contrast, Freundlich isotherm model is multilayer adsorption for heterogeneous nature of uneven size and shape of the adsorbent. In context, heterogeneous accessible sites yielded the best fit by the highest R^2 values.

3.5. Adsorption kinetics and mechanism

Kinetic modeling was performed with the help of experimental data retrieved from contact time for the various metal ion concentration. The pseudo-first-order and pseudo-second-order kinetic models [27] were used (Figs. 8–10) for this adsorption system. From kinetic models, the adsorption capacity and R^2 were calculated and tabulated (Tables 7–9). As a whole, the adsorption of Cd(II), Cu(II) and Ni(II) obeyed with pseudo-first-order kinetic model.

Adsorption mechanism was studied through the intraparticle diffusion model by analyzing the kinetic data. The linear equation derived from the plot between uptake q_t and the square root of time ($t^{1/2}$) indicates that if the linear lines pass through the origin, the intraparticle diffusion can be considered as the rate determining. This is well explained (Fig. 11) by the three stages of external surface adsorption, the gradual adsorption and finally equilibrium stage where intraparticle diffusion may become slower than the second step due to the lack of available active sites in the solution [27]. The intraparticle diffusion K_i values were obtained from the straight-line portions that increase with various solution temperatures. While increasing the temperature, pore diffusion

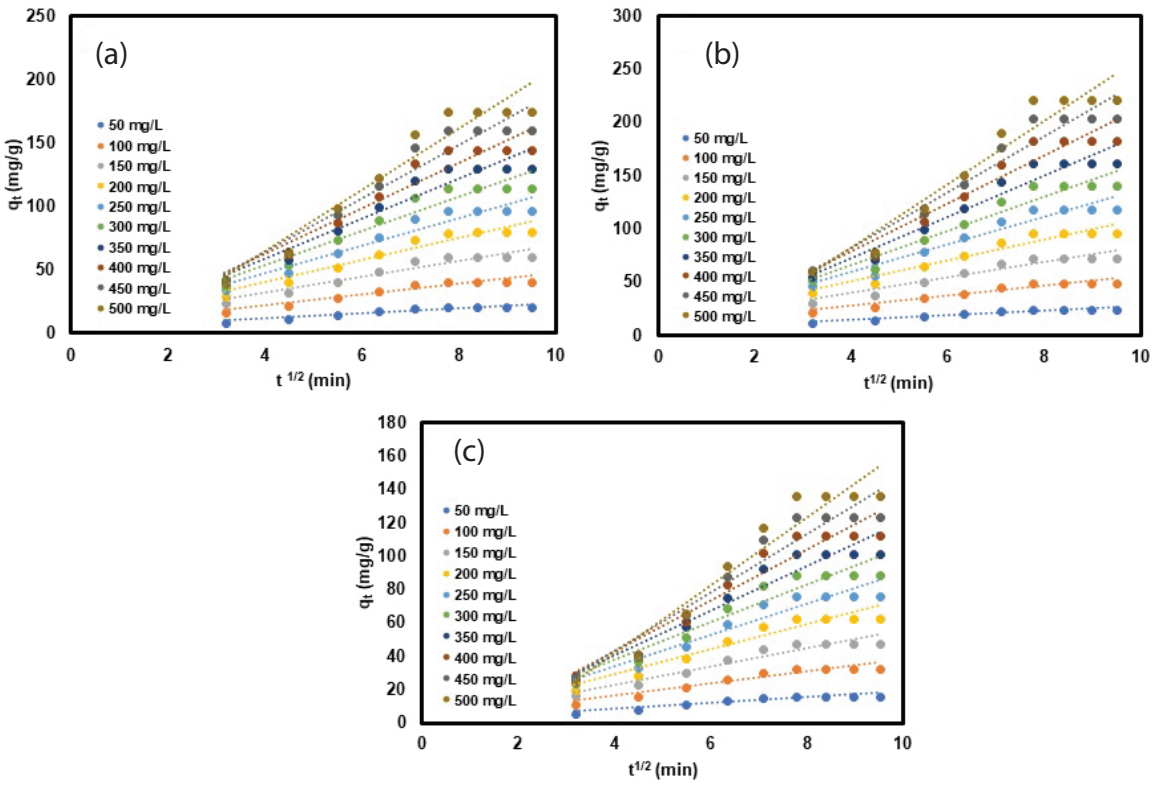

Fig. 11. Intraparticle diffusion model fit for the removal of (a) Cd(II), (b) Cu(II) and (c) Ni(II) ions (adsorbent dose = 2.4 g/L [Cd(II)], 2 g/L [Cu(II)] and 3 g/L [Ni(II)]; initial metal ion concentration = 50–500 mg/L; pH = 5.0; time = 10–90 min; and temperature = 303 K).

can also be promoted to enhance the rate of intraparticle diffusion whereas a large number of ions diffuse into the pores of adsorbent before being adsorbed. In addition, the linear lines do not pass through the origin, an evidence for the intraparticle diffusion model is not only the rate-limiting step [26,27].

4. Conclusion

In this research, the surface-modified agricultural waste biomass of JS was considered to be a potential adsorbent for the removal of Cd(II), Cu(II) and Ni(II) from the aqueous solution. The batch adsorption was monitored with the change in influential parameters such as the initial metal ion concentration, contact time and temperature. At optimized conditions, such as pH 5.0 at 303 K, the adsorption isotherm, kinetic and thermodynamic studies were carried out on the removal of metal ions. The experimental data were fit with the nonlinear isotherm models, whereas Freundlich and Redlich–Peterson models were observed with best fit by higher correlation coefficient. The maximum adsorption capacity of UMJS was 182.4, 259 and 140.9 mg/g for Cd(II), Cu(II) and Ni(II) ions, respectively. The pseudo-first-order kinetic model produced the best fit of experimental data. The thermodynamic parameters of $\Delta G°$, $\Delta H°$ and $\Delta S°$ resulted in the release of energy, spontaneous and exothermic in nature. Intraparticle diffusion model results showed that the particle diffusion is not the only rate-limiting step in this adsorption system. Finally, it was concluded that the prepared adsorbent can act as an effective adsorbent for the removal of toxic pollutants from the industrial wastewater.

References

[1] Z.A. Sutirman, M.M. Sanagi, K.J. Karim, W.A. Ibrahim, B.H. Jume, Equilibrium, kinetic and mechanism studies of Cu(II) and Cd(II) ions adsorption by modified chitosan beads, Int. J. Biol. Macromol., 116 (2018) 255–263.

[2] L. Li, F. Zhu, Y. Lu, J. Guan, Synthesis, adsorption and selectivity of inverse emulsion Cd(II) imprinted polymers, Chin. Chem. Eng. J., 26 (2018) 494–500.

[3] X. Sun, J. Zhu, Q. Gu, Y. You, Surface-modified chitin by TEMPO-mediated oxidation and adsorption of Cd(II), Colloids Surf., A, 555 (2018) 103–110.

[4] F. Liu, K. Zhou, Q. Chen, A. Wang, W. Chen, Preparation of magnetic ferrite by optimizing the synthetic pH and its application for the removal of Cd(II) from Cd-NH_3-H_2O system, J. Mol. Liq., 264 (2018) 215–222.

[5] J. Zhao, Y. Niu, B. Ren, H. Chen, Y. Zhang, Synthesis of Schiff base functionalized superparamagnetic Fe_3O_4 composites for effective removal of Pb(II) and Cd(II) from aqueous solution, Chem. Eng. J., 347 (2018) 574–584.

[6] J. Silva-Yumi, M. Escudey, M. Gacitua, C. Pizarro, Kinetics, adsorption and desorption of Cd(II) and Cu(II) on natural allophane: effect of iron oxide coating, Geoderma, 319 (2018) 70–79.

[7] T. Divisekara, A.N. Navaratne, A.S.K. Abeysekara, Impact of a commercial glyphosate formulation on adsorption of Cd(II) and Pb(II) ions on paddy soil, Chemosphere, 198 (2018) 334–341.

[8] I. Langmuir, The adsorption of gases on plane surface of glasses, J. Am. Chem. Soc., 40 (1918) 1361–1403.

[9] H.M. Freundlich, Over the adsorption in solution, J. Phys. Chem., 57 (1906) 385–470.

[10] O. Redlich, D.L. Peterson, A useful adsorption isotherm, J. Phys. Chem., 63 (1959) 1024–1026.

[11] J. Toth, C. Acta, State equations of the solid-gas interface layers, Acad. Sci. Hung., 69 (1971) 311–328.

[12] S. Guo, P. Jiao, Z. Dan, N. Duan, W. Gao, Synthesis of magnetic bioadsorbent for adsorption of Zn(II), Cd(II) and Pb(II) ions from aqueous solution, Chem. Eng. Res. Des., 126 (2017) 217–231.

[13] S. Suganya, P.S. Kumar, Influence of ultrasonic waves on preparation of active carbon from coffee waste for the reclamation of effluents containing Cr(VI) ions, J. Ind. Eng. Chem., 60 (2018) 418–430.

[14] C. Hu, P. Zhu, M. Cai, H. Hu, Q. Fu, Comparative adsorption of Pb(II), Cu(II) and Cd(II) on chitosan saturated montmorillonite: kinetic, thermodynamic and equilibrium studies, Appl. Clay Sci., 143 (2017) 320–326.

[15] A.K. Thakur, G.M. Nisola, L.A. Limjuco, K.J. Parohinog, W.J. Chung, Polyethylenimine-modified mesoporous silica adsorbent for simultaneous removal of Cd(II) and Ni(II) from aqueous solution, J. Ind. Eng. Chem., 49 (2017) 133–144.

[16] F.S. Hoseinian, B. Rezai, E. Kowsari, M. Safari, Kinetic study of Ni(II) removal using ion flotation: effect of chemical interactions, Miner. Eng., 119 (2018) 212–221.

[17] S. Suganya, P.S. Kumar, Kinetic and thermodynamic analysis for the redemption of effluents containing Solochrome Black T onto powdered activated carbon: a validation of new solid-liquid phase equilibrium model, J. Mol. Liq., 259 (2018) 88–101.

[18] Z.N. Garba, I. Ugbaga, A.K. Abdullahi, Evaluation of optimum adsorption conditions for Ni(II) and Cd(II) removal from aqueous solution by modified plantain peels (MPP), BENI-SEUF Univ. J. Appl. Sci., 5 (2016) 170–179.

[19] L. Wang, D. Hu, X. Kong, J. Liu, C. Zhou, Anionic polypeptide poly(γ-glutamic acid)-functionalized magnetic Fe_3O_4-GO-(o-MWCNTs) hybrid nanocomposite for high-efficiency removal of Cd(II), Cu(II) and Ni(II) heavy metal ions, Chem. Eng. J., 346 (2018) 38–49.

[20] O. Rahmanian, M. Maleki, M. Dinari, Ultrasonically assisted solvothermal synthesis of novel Ni/Al layered double hydroxide for capturing of Cd(II) from contaminated water, J. Phys. Chem. Solids, 110 (2017) 195–201.

[21] C. Cheng, J. Wang, X. Yang, A. Li, C. Philippe, Adsorption of Ni(II) and Cd(II) from water by novel chelating sponge and the effect of alkali-earth metal ions on the adsorption, J. Hazard. Mater., 264 (2014) 332–341.

[22] S. Guo, N. Duan, Z. Dan, G. Chen, W. Gao, g-C_3N_4 modified magnetic Fe_3O_4 adsorbent: preparation, characterization, and performance of Zn(II), Pb(II) and Cd(II) removal from aqueous solution, J. Mol. Liq., 258 (2018) 225–234.

[23] M. Fawzy, M. Nasr, S. Adel, H. Nagy, S. Helmi, Environmental approach and artificial intelligence for Ni(II) and Cd(II) biosorption from aqueous solution using *Typha domingensis* biomass, Ecol. Eng., 95 (2016) 743–752.

[24] M. Arshadi, M.J. Amiri, S. Mousavi., Kinetic, equilibrium and thermodynamic investigations of Ni(II), Cd(II), Cu(II) and Co(II) adsorption on barley straw ash, Water Res. Ind., 6 (2014) 1–17.

[25] L. Zeng, Y. Chen, Q. Zhang, X. Guo, J. Luo, Adsorption of Cd(II), Cu(II) and Ni(II) ions by cross-linking chitosan/rectoritenano-hybrid composite microspheres, Carbohydr. Polym., 130 (2015) 333–343.

[26] W. Sun, B. Jiang, F. Wang, N. Xu, Effect of carbon nanotubes on Cd(II) adsorption by sediments, Chem. Eng. J., 264 (2015) 645–653.

[27] A.A. Taha, M.A. Shreadah, A.M. Ahmed, H. F. Heiba, Multi-component adsorption of Pb(II), Cd(II), and Ni(II) onto Egyptian Na-activated bentonite; equilibrium, kinetics, thermodynamics, and application for seawater desalination, J. Environ. Chem. Eng., 4 (2016) 1166–1180.